A Comprehensive Integrity Verification Architecture for On-Airport LAAS Category III Precision Landing

Sam Pullen, Boris Pervan, Per Enge, and Bradford Parkinson
Department of Aeronautics and Astronautics, Stanford University

(Presented at **ION GPS-96** Conference, Kansas City, MO., Sept. 17-20, 1996)

BIOGRAPHIES

Sam Pullen, an S.B. Graduate of MIT, recently completed his Ph.D. in Aeronautics and Astronautics at Stanford University, where he is now a Research Associate. His research includes spacecraft design for reliability and robust control design along with studies of aircraft DGPS performance and integrity.

Boris Pervan, a graduate of Notre Dame and CalTech, completed his Ph.D. in Aeronautics and Astronautics at Stanford University. He is now a Research Associate at Stanford with a primary research focus on LAAS.

Per Enge is a Research Professor of Aeronautics and Astronautics at Stanford University. A Ph.D. graduate of the University of Illinois, his research focuses on DGPS aircraft landing applications. He previously taught at WPI and is an ION Satellite Division ex-Chairman.

Brad Parkinson is a Professor of Aeronautics and Astronautics at Stanford University and is the program manager for the Gravity Probe B spacecraft. He served as the first Program Director of the GPS Joint Program Office and was instrumental in the system's development.

ABSTRACT

Future Local Area Augmentation System (LAAS) architectures will most likely be constrained to lie on airport property. Such a system must provide protection against rare events in the GPS Signal in Space (SIS) that pose danger to airborne users conducting Category III precision landings. By allowing the aircraft to combine ground integrity information with its own checks in order to make the final integrity decision, LAAS should be able to meet the performance, integrity, continuity, and availability (PICA) requirements for this application.

Stanford has proposed a solution that includes internally redundant airport pseudolites (APL's) and a set of differential reference and monitor receivers connected to a central processing facility. Ground monitoring in-cludes comparisons of the code and carrier measurements at spatially separated monitors. Satellites and corrections with excessive discrepancies are eliminated, and the rest are uplinked to the aircraft as valid for use. Aircraft receiving the LAAS message compute the achievable bound on vertical error that determines whether approaches can commence or continue. Aircraft also perform space segment and redundant-channel consistency checks during their approach to detect any remaining errors in the Signal-in-Space (SIS).

The elements of this integrity architecture should combine to provide acceptable PICA availability for precision landings. Further refinements will focus on detailed specification of the aircraft VPL probability computation and mitigation steps, APL self-monitoring, and the use of Signal Quality Monitoring (SQM) to improve ground and airborne receiver robustness.

1.0 Introduction

The Local Area Augmentation System (LAAS) is designed to provide sufficient availability of accuracy, continuity, and integrity to satisfy the demanding requirements of aircraft precision approach, landing, and surface navigation under poor visibility. Use of the GPS constellation alone is not practical because the satellites do not provide sufficient ranging accuracy on their own and because there are too few of them to provide 99.9% availability. LAAS provides reference receivers at each airport to provide DGPS corrections to airborne code and carrier measurements. Airport pseudolites (APL's) are provided to improve positioning geometry and to allow improved accuracy from differential carrier phase processing as the aircraft approaches touchdown [3].

This section briefly introduces a proposed LAAS architecture composed of ground reference/monitor receivers, pseudolites, and a central processor and VHF transmission facility. It also explains the means by which integrity monitoring responsibility is shared between the ground and airborne elements of the system. Section 2.0 outlines sources of hazardous failures within the LAAS ground, air, and space segments. Sections 3.0, 4.0, and 5.0 detail the ground and airborne monitoring algorithms used to insure adequate protection against threats emanating from these three system branches. Section 6.0

draws conclusions from our preliminary results and points to important developments foreseen for the future.

1.1 A Preliminary LAAS Architecture

Figure 1 shows a proposed layout for the LAAS on-airport ground elements. This architecture uses the "Intrack APL" concept (two APL's at the opposite ends of a runway) to provide a differential-phase observable to aircraft approaching either runway end. Accuracy thus improves as aircraft approach the runway threshold, providing greater margin for integrity assurance at the most critical point in a Category III landing. Details of the processing and performance improvements attained from the Intrack APL concept are given in [3].

In addition, the need to provide accurate DGPS measurements from the ground that are insensitive to failures of a single ground receiver requires a network of redun-dant GPS ground receiver/monitors, or "ground moni-tors" (GM's) for short. As shown in Figure 1, these need to be spread out along a long baseline if the ground attempts to detect satellite ephemeris errors. Longer baselines are better for this purpose, but they would place more constraints on airport siting (see Section 5.2). The shorter baseline shown between GM's is needed to insure that multipath errors observed at the two separated antennas are statistically independent of each other. This separation is likely to be 30-100 m [4].

*1.2 Distributed Ground/Air Responsibility via **G**(x)*

Because of the limitations of GPS code measurement accuracy, it is difficult in some cases for the LAAS ground system to verify that sufficient navigation integ-rity exists for all airborne users. In some cases, this is difficult because of limited geometric observability on the ground; in others, it is due to the need to assess integrity based on the worst possible case for all aircraft in the terminal area. These concerns can be alleviated by allowing each aircraft to make its own final integrity determination using a pre-specified algorithm. In the GPS context, this philosophy has been termed "**G**(*x*)", which is shorthand for that algorithm [5].

The integrity paradigm on which ILS and other navigation aids are built assumes that the system insures its own integrity with integral monitoring systems that can clearly determine when the system is outside its specification. Users who receive valid information from it can thus assume it is safe to use. In a **G**(*x*) approach, the ground (or system provider) retains full responsibility for the integrity of the system, but the final determination of integrity for each approach may be made in each of the redundant sets of navigation avionics on the aircraft. The means by which this is done for our proposed architecture are detailed in Sections 3.0, 4.0, and 5.0.

2.0 Integrity Threat Sources and Causes

It is difficult to comprehensively monitor the GPS Signal-in-Space (SIS) at a single point in the processing

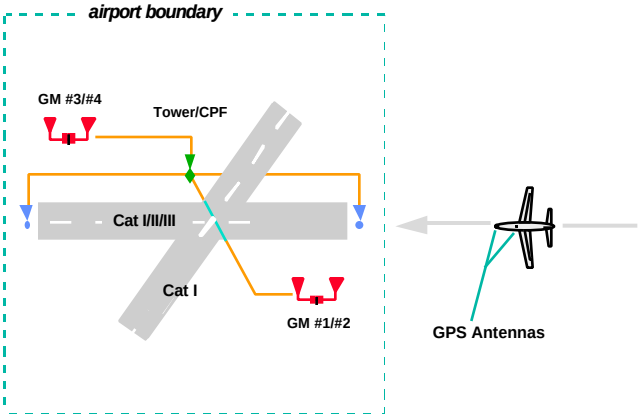

Figure 1: LAAS Intrack APL Architecture

tree because of the distributed activities of the ground, air, and space segments of a LAAS architecture. Figure 2 shows a diagram of the events that could lead to hazardously misleading information (HMI) for airborne users [2]. The probabilistic "tail" distribution of normal conditions allows for a small probability of HMI with no system failure. Failure events which could lead to HMI are broken down below.

2.1 Ground Segment Failures

The LAAS ground segment is made up of redundant GPS reference receiver/ground monitors (GM's), airport pseudolites (APL's), and a VHF data link (VDL) and associated monitor. Individual GM's could fail on some or all of their internal GPS receiver channels, and the resulting errors in the DGPS message would directly influence user navigation solutions. This failure mode is what drives the need for redundant (more than one) GM's with which to detect and isolate a failed GM. Redundant GM information also allows a quality statistic to be sent to the aircraft for each GPS satellite visible to the ground monitor network.

The LAAS ground segment also supplies the VHF datalink and APL transmissions. Ground messages computed at the central processing facility (CPF) could be incorrectly generated or received by airborne users. APL's that transmit additional GPS ranging signals from the ground must be monitored for hazardous errors similar to those that could result from the GPS satellites. If APL transmissions are RF-cabled or transmitted back to the GM network, DGPS corrections and GM comparisons can be done in the same manner as the satellites. However, it is desirable for the APL's to be independent of the GM network, so they may need to be self-monitoring (see Section 3.3).

Finally, the possibility of hazardous errors due to deliberate tampering with or spoofing of the system cannot be ignored. However, the distributed nature of GPS makes it difficult to produce hazardous ranging signals that are self-consistent inside the receiver. It is believed that LAAS will be at least as hard to spoof or tamper with as ILS landing systems are today; thus this is not yet a major area of concern.

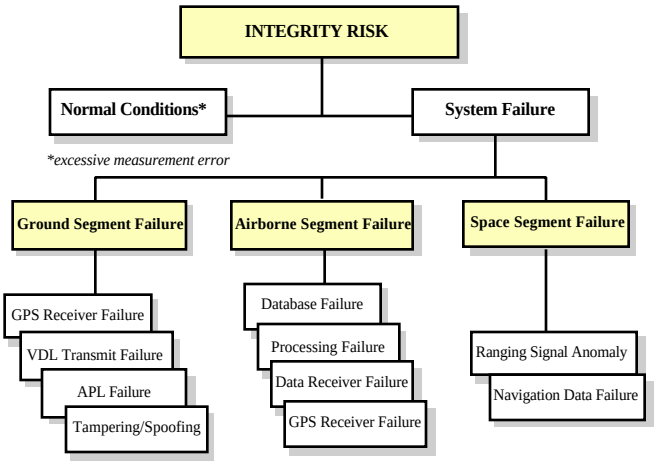

Figure 2: LAAS Integrity Fault Tree

2.2 Space Segment Failures

Individual satellite ranging signals may contain flaws that do not meet the SPS signal specification assumed in the LAAS requirements [1]. In the vast majority of cases, these errors will be calibrated out by the DGPS correction message because they affect reference and user equally. A large satellite clock offset that does not change faster than Selective Availability (SA) is an example of an error that is fully mitigated by DGPS. Only errors that are spatially or temporally decorrelated between GM network and airborne user would be threatening.

Figure 2 lists two space segment failure classes that could lead to HMI at the user. If clock errors in the ranging signal change too rapidly for DGPS to be able to predict an epoch or two ahead (to remove latency at the aircraft), user clock corrections could become erroneous. Also, if the ephemeris message gave a satellite position that had a large error in the direction parallel to the vector between GM reference point and user, significant user biases could result [12]. The LAAS service provider is responsible for mitigating these failures, but the ground segment may not be able to do it alone.

2.3 Airborne Segment Failures

Since the LAAS ground network cannot check aircraft errors in real-time, allocations must be made such that the ground can assume a minimal level of performance in its airborne integrity assessment. The same error budget is also applied by the aircraft when it evaluates real-time integrity using $\mathbf{G}(x)$. Hardware and processing failures that lead to hazardous failures in the aircraft (e.g., in the airborne data receiver or the central processor) are covered by specifying limits on the probabilities of these events such that they fall within the total airborne integrity allocation of 10^{-9} per approach [1].

Hazardous failures that occur in the processing of GPS observations need to be mitigated separately because their probabilities may exceed the integrity requirement. Cycle slips are generally detected within receivers, and airborne multipath (uncorrelated with the ground) is limited by the rapidly-changing dynamics of flight and the close proximity of on-aircraft reflective surfaces [10]. The aircraft has redundant airborne sensor (RAS) channels and can detect and eliminate failures that occur in only one GPS receiver/processor. Only failures that would appear on all sensor channels are major causes for concern.

3.0 Ground Integrity Monitoring

As discussed in Section 2.0, the primary purpose of ground monitoring is to remove failures in the ground segment itself, including internal reference receiver failures and external multipath. Three or more spatially separated GM's are needed to provide enough redundancy to be able to detect and isolate a single failed GM while providing valid ground measurements for airborne use. Figure 3 illustrates the ground processing steps from GM measurements to VHF data message broadcast.

To simplify processing and airborne use of the independent GM measurements, two preliminary transformations are made. First, a single-channel GPS signal generator is used to provide a reference clock for all GM's. GM code and carrier measurements PR and ϕ, from other ranging sources (SV's and APL's) $i = 1,\ldots, n$ are differenced from the signal generator measurement (denoted as ranging source 0) to eliminate the unknown clock offsets in each GM $j = 1,\ldots, m$ [6]:

$$\begin{aligned} P\hat{R}_j^i &= PR_j^i - PR_j^0 \\ \hat{\phi}_j^i &= \phi_j^i - \phi_j^0 \end{aligned} \qquad (1)$$

Second, the code and carrier measurements at each GM site are corrected to bring them to a "virtual reference point" on airport property. Each GM range measurement thus needs to be corrected for the known difference in effective range to the satellite in question as follows [2]:

$$\begin{aligned} P\tilde{R}_j^i &= P\hat{R}_j^i - e_j^i \cdot b \\ \tilde{\phi}_j^i &= \hat{\phi}_j^i - e_j^i \cdot b \end{aligned} \qquad (2)$$

where $P\hat{R}$ and $\hat{\phi}$ are the single-differenced (from (1)) code and carrier measurements at GM j, $P\tilde{R}$ and $\tilde{\phi}$ are the effective measurements for the virtual reference site, e_j^i is a line-of-sight unit vector from GM j to ranging source i, and b is the vector from GM location to virtual reference site. Both e and b are in expressed in local East-North-Up (ENU) coordinates. If the ranging source were not exactly where the navigation message indicated, a spatially-decorrelated error would result that is propor-tional to $\delta e \cdot b$, where δe is the 3-dimensional ephemeris error vector in the same ENU coordinate frame. Ephemeris errors of dangerous magnitude must be monitored for elsewhere in

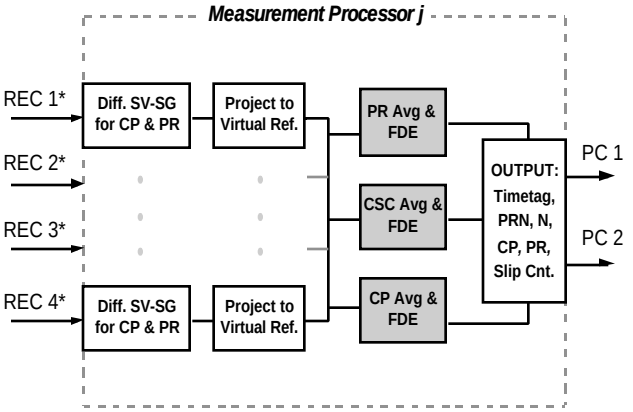

Figure 3: LAAS Ground Segment Processing

the architecture or be assumed to be less probable than the overall integrity requirement.

3.1 Ground Monitor Measurement Comparison

Once GM clock biases are removed, $P\tilde{R}$ and $\tilde{\phi}$ can be averaged across GM's to produce a mean ground measurement for each ranging source $i = 1,\ldots,n$:

$$P\bar{R}^i = \frac{1}{m}\sum_{j=1}^{m} P\tilde{R}_j \qquad \bar{\phi}^i = \frac{1}{m}\sum_{j=1}^{m} \tilde{\phi}_j \tag{3}$$

Preliminary detection and exclusion of ground-receiver-referenced failures, such as carrier cycle slips and rare-event code multipath, can be performed at the ground measurement processor (as indicated in Figure 3). However, because the ground processor does not have definite knowledge of which satellites the airborne receivers are tracking or the real-time aircraft-APL relative geometry, a post-screening protection limit that is useful at the aircraft cannot be computed on the ground. Instead, ground-based screening is simply targeted toward the removal of *measurement outliers* that could lead to integrity risk aboard the aircraft.

The consistency of redundant ground receiver measurements is most conveniently observed in parity space [2]. In this case, the stack of n raw (code and carrier) or processed (carrier-smoothed code) measurements for each satellite is pre-multiplied by the left nullspace of the observation matrix $|1 \cdots 1|^T$ to produce a parity vector p with $n-1$ elements. Under normal error conditions (i.e., no failures) the normalized parity vector magnitude $|p|/\sigma$ is a Chi-Square distributed random variable with $n-1$ degrees of freedom (where s is the standard deviation of the class of measurement under consideration). Thus, a detection threshold may be set on $|p|/\sigma$ to produce any desired probability of false alarm under normal error conditions. Using the limiting LAAS Category III navigation continuity requirement of 10^{-7} over a 30 sec exposure time and taking the maximum number of uncorrelated ground measurement epochs per approach to be 500 (consistent with a 2 Hz sample rate over the LAAS-specified Category IIIb approach duration of 230 sec [1]), a detection criteria of $|p|/\sigma > 7$ is selected.

Once a failure is detected for a particular satellite measurement set, it may also be possible to identify and remove the specific reference receiver channel responsible for the failure. At this point, we explicitly assume that the probability of more than one reference receiver failing simultaneously at a given measurement epoch is negligible. Using Bayes' Rule, the probability of a failure on reference receiver j $\left(REF_j\right)$ for the spacecraft under consideration can be written as:

$$\Pr\left(REF_j \mid p\right) = \frac{\Pr\left(REF_j\right) f\left(p \mid REF_j\right)}{\sum_{i=1}^{m} \Pr\left(REF_i\right) f\left(p \mid REF_i\right)} \tag{4}$$

3.2 Detection/Isolation of Failed Monitor Channels

A simple identification algorithm that maintains high integrity (by repressing mis-identification) would isolate reference measurement j if:

$$\Pr\left(REF_j \mid p\right) > 1 - \varepsilon\ , \tag{5}$$

where ε is set at 10^{-7} to provide an integrity risk per approach of 10^{-10}, under the conservative assumption that the prior probability of failure per approach is lower than or equal to 10^{-3}. Once a failure is isolated for a particular

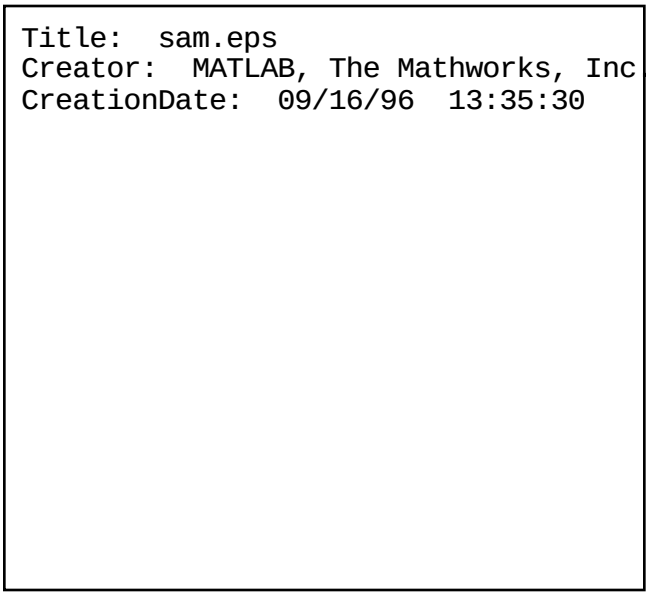

Figure 4: Ground Detection/Isolation Envelopes

satellite/reference receiver channel combination and measurement type, all measurement types are flagged unusable for that satellite/reference receiver channel combination for the remainder of one pre-specified Cat. IIIb approach duration of 230 sec. If a failure is detected, but (5) does not evaluate true for any reference receiver, the satellite measurement is declared unusable on all reference stations. Finally, if (5) evaluates true on one reference station for more than one satellite during any 230 second interval, all measurements from the affected receiver are declared unusable for an additional 230 seconds. These exposure times from [1] will vary depending on the Category of precision approach.

It is shown in [2] that the isolation criteria (4)-(5) may be practically implemented by applying limiting-case uniform bias distributions. For the quantitative thresholds given above, Figure 4 illustrates the resulting detection and isolation envelopes. Note that the choice of $|p|/\sigma > 7$, shown here by the inner circle detection zone radius, intersects the inner edges of the isolation envelope. This has the beneficial effect of minimizing the likelihood of a detected failure that cannot be isolated via (5), which would force the ground to remove that ranging source. Instead, the protection limit probability check on the aircraft (developed in Section 4.2) is used to evaluate these marginal cases.

3.3 APL and VHF Data Link Monitoring

In addition to handling failures within the reference receiver network, the LAAS ground segment must also insure the integrity of airport pseudolite (or APL) signals and the VHF data link broadcast from the airport. APL's are needed to provide Cat. III service under the intrack APL architecture, and they may also be used for carrier-smoothed-code systems to enhance availability. If pseudolites with "free-running" clocks are used, the GM network must provide corrections and failure screening for them just as they do for the satellites. This requires RF-cabling each APL back to each ground monitor and may be difficult or expensive to implement, since the cables may need to be several kilometers long.

A more versatile solution is the so-called "synchrolite" APL, which re-transmits received satellite signals with new PRN's so that aircraft users can directly difference the APL signal from the direct satellite signal [8]. This eliminates the need for ground measurements, but the APL must self-verify that it is sending a safe signal. A monitor receiver within the APL can receive both satellite signals and re-transmitted APL signals so that received-to-retransmit signal phase consistency can be monitored to within a few tenths of a meter. The details of this procedure are now under development.

The integrity of the VHF data transmission from the ground segment can be monitored both on the ground and in the air. The ground segment can use a far-field VHF monitor to confirm that the signal can be received and that the transmission matches the intended broadcast message. In addition, the aircraft confirms the integrity of each received message via the 32-bit CRC attached to each broadcast. This should insure that the data link meets the integrity requirement, but the data link poses a continuity threat if aircraft suffer VHF outages that exceed the time-to-alarm requirement of two seconds.

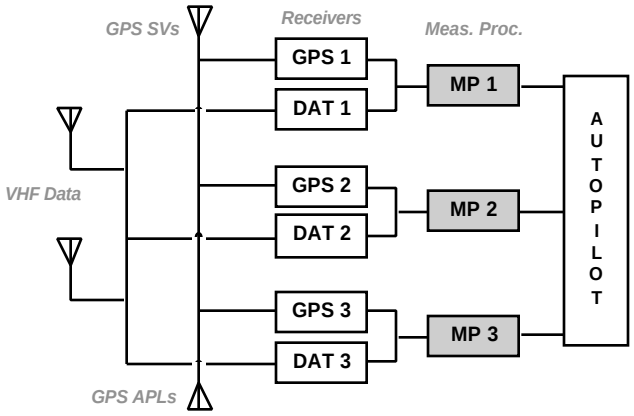

Figure 5: Triplex Aircraft Architecture

4.0 Airborne Integrity Monitoring

As illustrated in Figure 2 and Section 2.3, the aircraft is sensitive to undetected ground and space segment failures modes as well as failures occurring within the aircraft. Failure mitigation occurs via $\mathbf{G}(x)$ within each airborne receiver but also depends on the internal failure detection capability of each receiver and the redundancy provided by having more than one LAAS sensor track.

4.1 Redundant Airborne Sensor Channels

Figure 5 illustrates a typical arrangement of redundant sensor channels feeding into an aircraft autopilot. In the triplex configuration shown here, three independent GPS and VHF receivers provide processed measurements to the autopilot in the form of ILS deviations. This is included in a separate $\mathbf{G}(x)$ algorithm for each channel that also performs its own integrity checks. The autopilot uses its own fault-detection and isolation algorithm to throw out a channel that disagrees with the other two by more than a pre-set threshold. While these thresholds and the exact logic used are not public, they do constrain the accuracy of the individual airborne channels and provide substantial mitigation of failures that are not correlated across receiver channels.

4.2 Aircraft VPL Probability Computation

In addition to providing ILS position deviations, each sensor track executes its own $\mathbf{G}(x)$ algorithm to confirm that each approach meets the integrity requirement before the approach (for availability determination) and all the way to touchdown. This is done primarily by computing the probability that the unknown position error is

bounded within specified limits. Larger errors constitute "hazardously misleading information", or HMI, whose probability must lie below 1 in a billion per approach according to existing ICAO requirements and the LAAS ORD [1]. Both vertical and horizontal error bounds must be checked, but for LAAS, the vertical dimension is more challenging until the aircraft touches down.

The probability of vertical error (denoted by R_V) exceeding a specified vertical protection limit, or VPL, can be estimated on the aircraft if the VHF data message includes the measurements of all ground monitors that pass the ground screening procedure of Section 3.0 (these are denoted as $\mathbf{e}_g$). This is done by breaking down that probability among the possible failures as follows:

$$\Pr[R_V > VPL] = \Pr[R_V > VPL \mid H_o, \mathbf{e}_g] \Pr[H_o] + \sum_{k=1}^{m} \Pr[R_V > VPL \mid H_k, \mathbf{e}_g] \Pr[H_k] \quad (6)$$

where H_o stands for the normal-case hypothesis: each GM's corrections are assumed to be Gaussian with mean 0 and variance σ_g^2, and H_k stands for a bias failure on GM k, where $k = 1,\ldots, m$. The terms $\Pr[H_o]$ and $\Pr[H_k]$ represent the prior probabilities of these cases. The probability of failure H_k for any given GM, after large errors are screened out by the ground segment, is conservatively assigned to be 10^{-5} per approach, leaving the remainder, $1\text{-}10^{-5}m$, as the probability of case H_o. Note that these probabilities can be updated based on the ground measurements using the procedure of Section 3.1.

The ground measurements are used to compute the probability that position error exceeds the vertical and horizontal protection limits *for the most critical point in the approach*. At each epoch, each aircraft channel uses the code and carrier measurements from each individual GM k with its own measurements to compute a position fix x_k. The m different position fixes are averaged to get the position x for that channel and are also processed under each of the m+1 failure hypotheses for the purposes of (6). Under case H_o, the probability that the averaged position x (computed from all m GM's) is assumed to be Gaussian with bias zero and variance (for vertical error):

$$\sigma_{H_o}^2 = VDOP^2 \left[\sigma_a^2 + \frac{\sigma_g^2}{m}\right] \quad (7)$$

where σ_a is the airborne ranging standard deviation and *VDOP* includes the effects of intrack-APL code/carrier processing where applicable (under carrier-smoothed code, it is the normal satellite geometry calculation augmented with any APL's) [3]. Under any of the failure cases $H_1,\ldots,H_m$, the bias B is non-zero because the aircraft is including a biased GM in its position averaging:

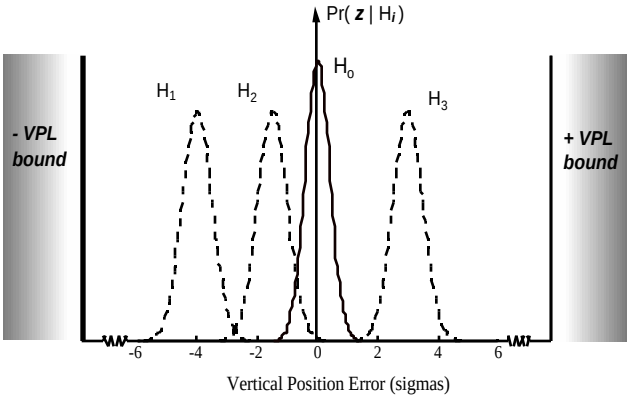

Figure 6: Vertical Error Distibutions

$$B_{H_k} = R_o - R_k \quad (8)$$

where R_o is the vertical position solution averaged over all m ground monitor measurements and R_k is the solution averaged over all GM's except GM k. In the carrier-smoothed code case, the bias can be computed by:

$$\hat{B}_{H_k} = \sum_{i=1}^{n} \left[\mathbf{G}^+[3,i]\left(z_{o,i}/m - z_{k,i}/(m-1)\right)\right] \quad (9)$$

where $z_{k,i}$ is the sum of all SV i GM code measurements except for GM k (if $k > 0$) and $\mathbf{G}^+$ is the pseudoinverse of the satellite/APL direction cosine geometry matrix [12]. The variance in each failure case is given by:

21 Healthy GPS Satellites

	# APL's	VDOP bound	VDOP avail.	min. VPL (m)
Cat. I	0	8.2	0.9863	14.0
	1	8.2	0.9991	12.0
	2	8.2	1.0000	10.0
Cat. II	0	3.6	0.9382	7.5
	1	3.6	0.9941	7.5
	2	3.6	0.9977	6.0
Cat. IIIb	2 (intrk)	4.3 (sub)	0.9510	5.0

$$\sigma_{H_k}^2 = VDOP^2 \left[\sigma_a^2 + \frac{\sigma_g^2}{m-1}\right] \qquad k = 1,2,\ldots,m \quad (10)$$

These results give Gaussian distributions for the probability that vertical error R_V exceeds a specified VPL:

$$\begin{aligned} \Pr[R_V > VPL \mid H_o] &\sim Gaussian\left(\mu = 0, \sigma^2 = \sigma_{H_o}^2\right) \\ \Pr[R_V > VPL \mid H_k] &\sim Gaussian\left(\mu = B_{H_k}, \sigma^2 = \sigma_{H_k}^2\right) \end{aligned} \quad (11)$$

Figure 6 shows these distributions and illustrates how each hypothesis is evaluated relative to the VPL limit.

If the VPL requirement cannot be met using all range measurements and GM's, the process can be redone after removing the most troublesome elements. The first step would be to remove the GM k (if $m > 2$) whose probability of exceeding VPL under H_k from (11) is the largest. If this is not successful in reducing $\Pr[R_V > VPL]$ below 10^{-9}, each of the n ranging sources can be removed one-by-one from **G** and the process redone n times to find the n-1 case whose VDOP and probability of exceeding VPL meets the requirements (this requires n "subset" computations of $\mathbf{G}^+$). Isolating more than one ranging source (or a ranging source and a GM) is likely to be impractical. These isolation steps are illustrated in Figure 7. Note that separate filters may need to run concurrently to allow rapid isolation in the case of intrack APL code-carrier processing [3].

This approach has two key advantages. One, it allows the aircraft to combine ground measurements with its own satellite and APL geometry to verify integrity at any point in the approach, avoiding the need for the ground segment to check all possible cases of satellite and APL visibility and determine which are acceptable. Second, the VPL check on the aircraft can determine which off-nominal cases are hazardous and which pose no threat. This allows ground screening to be less conservative.

4.3 VPL Availability Simulation Results

Since the integrity algorithm outlined here tracks ground and airborne error estimates into probabilities of exceeding a specified allowable VPL, the first step in evaluating it is to simulate worst-case ground and airborne biases along with normal-case errors to ensure that VPL falls within the bounds for system availability.

GPS geometries under two outage conditions, 24 healthy GPS satellites and 21 out of 24 satellites, have been simulated for the Cat. I, II, and IIIb cases with 0, 1, and 2 (required for Cat. III in-track) APL's and $m = 3$ GM's. Normal-case ground and aircraft receiver noise has been estimated as $\sigma_g = \sigma_a$ 0.25 m with 20-second carrier

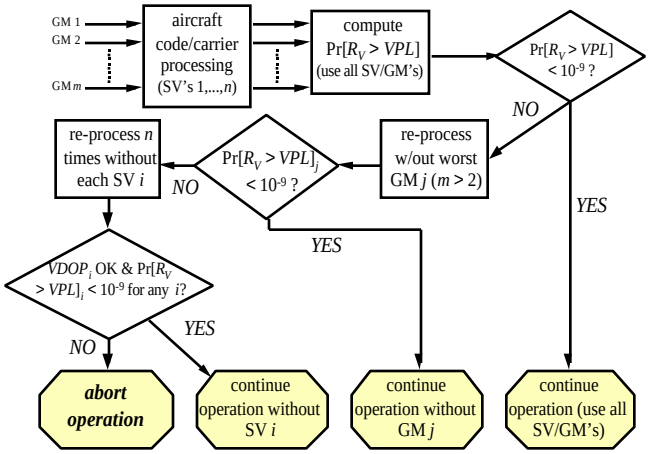

Figure 7: VPL Isolation Process

smoothing (inside the receiver) [5,6]. The worst-case bias allowed by ground screening is $7\sigma_g$ = 1.75 m (see Section 3.1). This bias is placed on one failed GM when the failure cases H_k (k=1,...,m) are evaluated. For a failed GM, the worst-case, worst-direction bias is placed on each satellite with probability 0.02 given H_k,. With probability 0.98/n, each of the n ranging sources are separately assigned this worst-case bias. Normal receiver noise from (7) is modeled for the H_o case.

The above simulation thus evaluates the ability of ground-screening alone to provide sufficient availability provided that the probability of exceeding VPL is evaluated on the aircraft as in Section 4.2. Table 1 shows these availability results, summed over 10 large Cat. III airports across the Continental U.S. For each category of approach, a VDOP bound (worst subset VDOP for Cat. IIIb to meet the 10^{-7} continuity requirement over 30 seconds) is applied assuming carrier smoothed code, giving the availability results shown [1,13]. Probabilities of exceeding VPL are then computed for a range of VPL limits, and the one tabulated here is the lowest VPL bound that imposes no further availability penalty.

We see that availability is fine for approaches with 24 healthy satellites, although Cat. II falls short of 0.999 with no APL's. For 21 healthy SV's, Cat. I needs one APL to exceed 0.999, and Cat. II and III fall a little short even with 2 APL's. The VPL bounds that can be met with no availability penalty also worsen with only 21 healthy satellites. VPL bounds of 10 m for Cat. I are quite reasonable and lie well within the 19.2 m HMI bound for Category I using WAAS [14]. The Cat. II and III bounds may be acceptable under a future LAAS ORD, but they are not as tight as those for similar ILS approaches. However, these are upper bounds on achievable VPL because they allow no availability loss beyond the VDOP check and because they are based on worst-case biases after ground screening. Even under the worst case, these bounds can be further tightened by 1 m or so with only a 2-5% loss in availability.

When ground measurement errors are simulated from the above noise models, the advantages of this VPL calculation become more apparent. Simulations assume either the normal case, where only Normal(0,σ_g^2) errors are

24 Healthy GPS Satellites

	# APL's	VDOP bound	VDOP avail.	min. VPL (m)
Cat. I	0	8.2	1.0000	8.5
	1	8.2	1.0000	8.0
	2	8.2	1.0000	7.6
Cat. II	0	3.6	0.9929	6.0
	1	3.6	1.0000	
	2	3.6	1.0000	
Cat. IIIb	2 (intrk)	4.3 (sub)	0.9985	

Table 1: Worst-Case VPL Availability

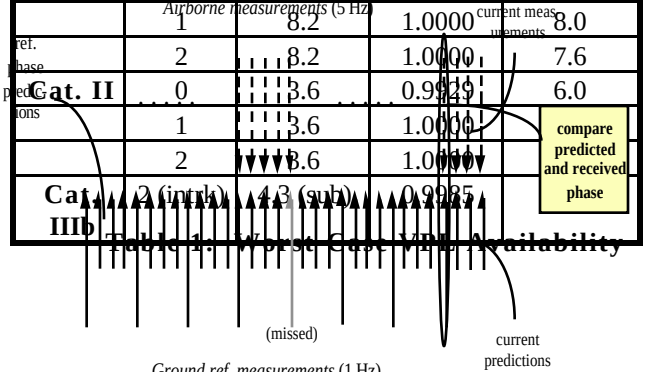

sampled on each GM, or a failure bias on one GM that affects either one or all ranging measurements as explained above. For Cat. IIIb, using actual noise samples under normal conditions improves the achievable VPL with zero availability penalty to 3.5 m. When worst-case biases from one GM failure are sampled on all n range measurements, no VPL under 7 m comes close to meeting the 10^{-9} probability that would allow the aircraft to complete the approach. The same is true for Cat. I and II: significant biases should always be flagged.

4.4 Aircraft Receiver Failure Mitigation

A key question is the degree to which cycle slips and large multipath or interference threaten safe navigation and how often they appear on more than one sensor channel. Dangerous errors on one receiver should be isolated out by the autopilot, and current GPS receivers should be very resistant to cycle slips of enough cycles to significantly bias the airborne processing because they include internal cycle-slip mitigation. In addition, recent studies of aircraft multipath indicate that unsmoothed airframe code multipath has a standard deviation of 20-30 cm, which falls to 5-10 cm with carrier smoothing or narrow-correlator receivers [10]. Thus, while this effect may be somewhat correlated across airborne channels, it should fit within a 25-30 cm 1σ airborne noise budget.

The only way to assess whether further mitigation of these failures is needed within $\mathbf{G}(x)$ is to determine the magnitude and likelihood of failures that could lead to hazardously misleading information via simulation and to inject the "most critical" of these into a GPS signal generator, which can test the intrinsic ability of the receiver and $\mathbf{G}(x)$ to resist them. Airborne failure modes are not currently seen as being design drivers for LAAS integrity, but if some are discovered in this way, additional mitigation would take the form of more stringent receiver specifications and cross-checking via RAIM or via jump detection as proposed in [6].

5.0 GPS Satellite Integrity Monitoring

The space segment failures mentioned in Section 2.2 are difficult to completely mitigate within the LAAS ground segment because their effects at the aircraft will differ from what is observed on the ground. While the ground can perform a useful screen against these events, the most effective course is to mitigate them on the aircraft as part of the "$\mathbf{G}(x)$" algorithm using separate checks for clock and ephemeris errors.

5.1 Spacecraft Clock Consistency Check

As discussed in Section 2.2, LAAS users must predict an epoch or two ahead to compensate for the delay in transmitting ground measurements. The clock model used for this update could be invalid in the case of a wildly erratic clock. Such a failure can be detected by comparing the most recent ground measurement with the one predicted by the model for that epoch.

For the Stanford LAAS architecture, a reference phase predictor was developed that fits a quadratic function of time to the last 7 measurements. These coefficients are sent to the aircraft, allowing it to compute a ground reference measurement for any aircraft timetag [9]. This approach has an rms error of 0.93 cm for a two-second-ahead prediction (the maximum allowed, since LAAS must satisfy a 2-second time-to-alarm requirement) [1]. Assuming that nominal performance is Gaussian, erratic clock errors in past data can be detected once they exceed 6σ, or about 5.6 cm, with acceptable false alarm rates.

Figure 8 illustrates this comparison with ground updates at 1 Hz and aircraft updates at 5 Hz. With 1 Hz updates, the 2-second time-to-alarm requirement allows only one ground message to be missed before the approach must be aborted. LAAS Cat. III continuity requirements would be violated in this case if the probability of two consecutive missed messages exceeds 10^{-7} over 30 seconds [1]. Therefore, if the datalink bandwidth allows, updates at 2 Hz would be preferable.

The advantage of doing this check on the aircraft is that the ground would not have to search the space of all possible outages to confirm that the satellite clock is safe. Instead, the ground segment, as part of its screening process, can perform this consistency check as when it computes the quadratic fit, thereby assuming that all ground messages are received by the aircraft. Satellites which cannot pass this "best-case" ground check can be eliminated right away. Each aircraft can then confirm this using the same process if messages were missed.

5.2 Spacecraft Ephemeris Error Check

As discussed in Section 2.2, satellite ephemeris errors with components parallel to the user-to-reference vector that are larger than 1-2 km can be dangerous to aircraft on precision approach. It may be possible for a failure to not be corrected by the GPS Master Control Station in time to prevent incorrect ephemeris messages from being broadcast from satellites flagged as healthy. In fact, an unconfirmed report of an apparent 30 km ephemeris error on SVN 37 from 1730 Zulu on March 29, 1996 is being investigated [15]. This satellite had an unsched-uled one-minute outage at 1646, suggesting that perhaps the error was noticed and corrected at that time [16]. Note that LAAS does not presume the use of a civilian integrity check for each satellite as will be done by the Wide Area Augmentation System (WAAS), although WAAS should quickly identify any significant ephemeris error from its widely-spread reference stations.

Range biases on satellites with undetected ephemeris errors grow with the separation from the reference point [12]. Two separated ground monitors can attempt to observe the ephemeris error by differencing code and carrier measurements between each other (after GM clock biases are removed in (1)). However, the maximum separation between two ground monitors is constrained by the airport

Figure 9a: Ephemeris Errors at Cat. III DH

dimensions, siting restrictions, and the need to run cables to distant locations on the airport.

Figure 9 contains the results of a simulation of satellite ephemeris errors as large as 100 km occurring on one satellite out of the set visible to a user at San Francisco Airport. The plots represent histograms (of 9.1 million samples) of the ideal (zero-noise) code-phase difference between two ground monitors separated by 3.1 km at San Francisco Airport (SFO) plotted against the post-correction range bias on the erroneous satellite. Results are shown for two locations along the Cat. III approach.

Figure 9a is the plot for the aircraft at the Cat. III decision height, which is about 1.9 km from the virtual reference point. In this case, the biases are on the order of several meters, and a 5-meter threshold on the code (pseudorange) difference between the two GM's will detect almost all dangerous vertical position errors. However, the biases are much greater in Figure 9b, where the aircraft is back at the beginning of the Cat. III approach, 10 kilometers from touchdown. In this case, range biases of many tens of meters could go undetected on the ground.

If a given satellite ephemeris error is not detected, the resulting bias can start out very large but will gradually decrease as the aircraft approaches the 100-foot altitude point defined to be the most critical point for LAAS. This clearly is a hazard, and the use of separated ground monitors to mitigate it will be highly airport-dependent. Fortunately, this risk can be practically eliminated by performing a carrier-phase RAIM check on the aircraft.

The use of RAIM on the aircraft to check for ephemeris errors is based on the "synthetic baseline concept" in which the aircraft builds its on baseline for ephemeris comparison as it moves down the approach path [11]. At selected points down the approach, each aircraft channel differences the current carrier phase from that of the initial fix at time t_o. This observation is represented by:

21 Healthy GPS Satellites

$$\bar{\phi}_t = \begin{bmatrix} \phi_t^{(1)} - \phi_{t_o}^{(1)} \\ \phi_t^{(2)} - \phi_{t_o}^{(2)} \\ \vdots \\ \phi_t^{(n)} - \phi_{t_o}^{(n)} \end{bmatrix} = \mathbf{G}u + \delta\mathbf{G}u + \delta\bar{\phi} \quad (12)$$

	Cat. I CSC	Cat. I + ERAIM	Cat. II CSC	Cat. II + ERAIM	Cat. IIIb
0 APL	1.0000	0.9990	0.9929	0.9919	N/A
1 APL	1.0000	1.0000	1.0000	1.0000	N/A
2 APL	1.0000	1.0000	1.0000	1.0000	0.9985

Table 2: Availability of Ephemeris RAIM

where u is the relative position solution, φ is the carrier phase measurement, and $\mathbf{G}$ is the $n \times 4$ geometry matrix from before. The carrier noise term on the right has 1σ error below 1 cm. Biases due to ephemeris errors would appear in the $\delta\mathbf{G}u$ term, where $\delta\mathbf{G}$ represents the error in the line-of-sight vector due to the ephemeris error. With $n > 4$ ranging sources in view, computing the residual:

$$r_t = \left(\mathbf{I}_n - \mathbf{G}\mathbf{G}^+\right)\bar{\phi}_t = \mathbf{S}\bar{\phi}_t \quad (13)$$

and comparing its magnitude:

$$\left|r_t\right| = \bar{\phi}_t^{\mathrm{T}}\mathbf{S}\bar{\phi}_t = \bar{\phi}_t^{\mathrm{T}}\left(\mathbf{I}_n - \mathbf{G}\mathbf{G}^+\right)\bar{\phi}_t \quad (14)$$

to a detection threshold $T \approx 6\sigma \approx 6$ cm will detect practically all single-satellite and almost all dual-satellite ephemeris errors of hazardous size [2]. The use of this test is constrained to the $n > 4$ case and requires that the detectable bias on the most sensitive satellite be smaller than the definition of hazardous position error. For this

Figure 9b: Ephemeris Errors at Approach Init.

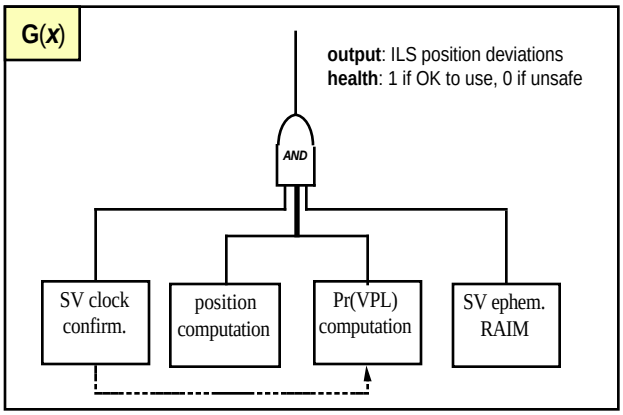

Figure 10: G(*x*) Processing Activities

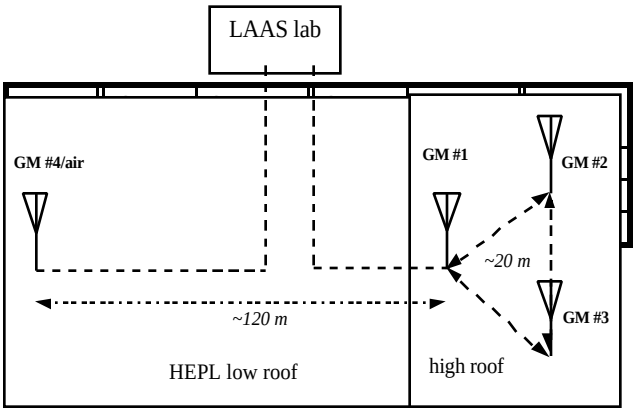

Figure 11: Stanford Ground Monitor Test Setup

latter requirement, a 3-meter protection radius and the 6-km airborne baseline mentioned below allow the maximum failure slope defined by [2,7]:

$$Max\ Vslope^2 = \max_{i=1,\ldots,n} \left(\frac{\mathbf{G}^+[3,i]}{\mathbf{S}[i,i]} \right) \qquad (15)$$

to be as large as 72. This requirement is met 90% of the time for five-satellite geometries and 99.98% of the time when 6 or more ranging measurements are present.

This RAIM check in the carrier domain provides a factor-of-30 improvement in ephemeris error observability compared to doing the check via code differences between two separated ground monitors (as in Figure 9). For example, if RAIM checks are done along the approach from 10 to 4 km from touchdown, the resulting maximum separation of 6 km is approximately equivalent to a 180-kilometer separation on the ground. This means that ephemeris error observability on the aircraft is much greater than could be achieved by separating two monitors within airport property.

5.3 Availability of Ephemeris RAIM

While relative RAIM checks on the aircraft are the best means of mitigating ephemeris errors for LAAS, an availability penalty is paid relative to carrier-smoothed code by itself, which does not necessarily require redundant measurements. If a simple availability-of-accuracy check is made for carrier-smoothed code without RAIM, Category I approaches may be allowed for four-satellite geometries with VDOP below 8.2 (see Table 1), which is the case in 80% of four-satellite geometries. However, the requirements are much tighter for Category II and III approaches, as was shown for VPL availability in Section 4.3. For Cat. IIIb, where one must assure that the loss of the worst-case satellite can be tolerated during the most critical 30 seconds, RAIM has no additional requirement because the RAIM check will be complete well before the landing threshold is reached. Note that these results are independent of that VPL calculation, as we are trying to isolate the penalty due to adding RAIM alone.

As before, these results, shown in Table 2, are broken down into simulations where all 24 GPS satellites are usable and ones where a randomly sampled 21 out of 24 are usable. The ephemeris RAIM check costs very little in terms of availability for Category II and III landings, where APL's are necessary to obtain decent availability in the 21-satellite case. The only case where a substantial difference exists is for Category I approaches with 21 satellites and no APL's, where the RAIM availability of 94% is lower than the basic carrier-smoothed code availability of above 98%. This would only be significant if 98% availability is all that would be needed, since APL's would be needed to make it near 99.9%, and in that case, the RAIM availability penalty is smaller.

*5.4 **G**(x) Integrity Algorithm Summary*

Figure 10 shows a simplified diagram of the elements of G(x) processing on each aircraft sensor channel. The primary tasks of airborne position processing and protection limit confirmation are shown in the center boxes. Separate checks of the consistency of each satellite clock and of ephemeris errors are shown on the sides. These space-segment checks in the aircraft augment ground screening and can be implemented either as a veto on safe performance (as shown by the "AND" gate in Figure 10 - all checks must be passed) or by including failure hypotheses in the protection limit calculation (note the dotted line from clock prediction to VPL probability check).

6.0 Conclusions and Further Work

In this paper, a preliminary LAAS integrity verification algorithm has been presented that is adaptable to both carrier-smoothed code and floating-point carrier cycle processing. In this concept, final availability and integrity decisions are made on the aircraft using a pre-specified "**G**(*x*)" algorithm based on inputs transmitted from the ground. The mathematical framework for the evaluation of the probability of exceeding allowed protection limits has been explained, and the probabilities of exceeding VPL using representative DGPS error models have been computed by simulation.

The algorithm proposed here is comprehensive, but it is far from complete. While the proposed method for ground screening of ranging sources and individual GM's is reasonably complete, the use of signal quality monitoring (SQM) inside the ground receivers should offer better rejection of anomalous signals before they are voted on by the CPF. Multipath mitigation techniques may also improve nominal signal performance and thereby improve the attainable protection levels. Self-monitored omni-markers promise much more flexible integration of APL's into the LAAS ground segment.

More work needs to be done on modeling GM receiver noise and statistical correlation (both spatial and temporal) in order to verify the performance of ground screening and the projection of probabilities of exceeding VPL. This is being done using the Stanford ground monitor network shown in Figure 11. This setup has three GM's that form a triangle and one GM further away that can also be used for static testing of the airborne algorithms. These four antennas are fed into two computers in the nearby LAAS lab which house four NovAtel 3951 GPSCard® receivers. This setup will measure the noise magnitude and statistical independence of these GM's in the high-multipath environment around these antennas and will serve as a test vehicle for ground monitoring algorithm refinement. In addition, more detailed simulations of precision approaches will be used to refine monitor thresholds along the lines of [7].

On the aircraft, a complete definition of the calculations and consistency checks to be included in "$\mathbf{G}(x)$" will have to be developed once the baseline LAAS architecture is chosen. This architecture will be intensively tested by simulations of failures and off-nominal performance in all three system segments to ensure that they are mitigated by the integrity processing chain so that all continuity and integrity requirements are met in an operational system.

ACKNOWLEDGMENTS

The authors would like to thank the following people for their help with this research: Dave Lawrence, Dr. Clark Cohen, Stu Cobb, Konstantin Gromov, Hui-Ling Lu, and Guttorm Opshaug. The advice and interest of many other people in the Stanford GPS research group is appreciated, as is funding support from the FAA and Boeing Commercial Airplane Group.

REFERENCES

[1] *LAAS Operational Requirements Document,* Change 1. Federal Aviation Administration, December 1995.

[2] B. Pervan, "Navigation Integrity for Aircraft Precision Approach using the Global Positioning System." Ph.D. Dissertation, Stanford University, SUDAAR 677, March 1996.

[3] D. Lawrence, B. Pervan, S. Cobb, C. Cohen, J. Powell, P. Enge, B. Parkinson, "Performance Evaluation of On-Airport Local Area Augmentation System Architectures", *Proceedings of ION GPS-96.* Kansas City, MO., Sept. 17-20, 1996.

[4] G. Courtney, Wilcox Electric Co., Telephone Conversation, August 29, 1996.

[5] B. DeCleene, *LAAS Architecture Review Committee Minutes*, McLean, VA., July 18-19, 1996.

[6] F. van Graas, *LAAS Architecture Review Committee Minutes*, McLean, VA., May 30-31, 1996.

[7] S. Pullen, "Probabilistic Engineering System Design: Applications to Spacecraft and Navigation Systems", Ph.D. Dissertation, Stanford University, SUDAAR 680, June 1996.

[8] S. Cobb, D. Lawrence, B. Pervan, , C. Cohen, J. Powell, B. Parkinson, "Precision Landing Tests with Improved Integrity Beacon Pseudolites", *Proceedings of ION GPS-95.* Palm Springs, CA., Sept. 12-15, 1995, pp. 827-833.

[9] D. Lawrence, B. Pervan, , C. Cohen, H.S. Cobb, J. Powell, B. Parkinson, "A Real-Time Architecture for Kinematic GPS Applied to the Integrity Beacon Landing System", *Proceedings of ION 51st Annual Meeting*. Colorado Springs, CO., June 5-7, 1995, pp. 271-280.

[10] T. Murphy, R. Snow, M. Braasch, "GPS Multipath on Large Commercial Transport Airframes", *Proceedings of ION 1996 National Technical Meeting*. Santa Monica, CA., Jan. 22-24, 1996, pp. 137-143.

[11] "Local Area Augmentation System (LAAS) Integrity Panel (LIP): Integrity Beacon Landing System (IBLS)." Department of Aeronautics and Astronautics, Stanford University, December 15, 1995.

[12] B. Parkinson, P. Enge, "Differential GPS," in B. Parkinson and J. Spilker, Eds., *Global Positioning System: Theory and Applications*. Washington, D.C.: AIAA, 1996. Volume II, Chapter 1, pp. 3-50.

[13] C. Shively, R. Braff, R. Swider, "LAAS Architecture - Preliminary Recommendations." FAA LARC Presentation to SOIT, August 15, 1996.

[14] "Wide Area Augmentation System (WAAS) Specification", Federal Aviation Administration, FAA-E-2892, Dept. of Transportation, May 9, 1994.

[15] M. Zeitzew, "OCS Performance Analysis", *Minutes of PAWG-96.* Colorado Springs, CO., August 22, 1996.

[16] NANU 063-96089, downloaded from *U.S. Coast Guard GPS Information Center*. Internet Address: http://www.navcen.uscg.mil/ gps/gps.htm